Developmental Biology **228,** 136–149 (2000)
doi:10.1006/dbio.2000.9931, available online at http://www.idealibrary.com on IDEAL®

The Complex Dynamic Network of Microtubule and Microfilament Cytasters of the Leech Zygote

Viviana Cantillana, Milena Urrutia, Andrea Ubilla, and Juan Fernández[1]
Department of Biology, Faculty of Sciences, University of Chile, Santiago, Chile

The organization of the cytoskeleton in the early first interphase zygote and its involvement in organelle redistribution were studied in the glossiphoniid leech *Theromyzon trizonare* by confocal and electron microscopy, immunofluorescence, and time-lapse video imaging after microinjection of labeled tubulin and/or actin and loading with a mitotracker. The cytoskeleton consists of an inner or endoplasmic and an outer or ectoplasmic domain. The inner domain consists of a monaster whose fibers retract from the zygote periphery by the end of the early first interphase. The outer domain is built upon a network of microtubules and microfilaments cytasters. Short pulses of microinjected labeled actin or tubulin and Taxol treatment demonstrate that cytasters are centers of microtubule and microfilament nucleation. Immunostaining with anti-centrophilin, anti-BX-63, and anti-AH-6 indicates that the network of cytasters includes centrosomal antigens. Cytasters move in an orderly fashion at speeds of 0.5–2 μm/min, in an energy-dependent process retarded and finally blocked by the ATP analogue AMP–PNP and high concentrations of Taxol. Colliding cytasters fuse and form larger cytoskeletal nucleation centers. The leech zygote is a highly compartmentalized cell whose cytasters function as articulated components of a very dynamic cytoskeletal system engaged in bulk transportation of organelles during ooplasmic segregation.

Key Words: **cytasters; leech zygote; mitochondria transport; zygote cytoskeleton; cytoskeleton assembly; cytoskeleton dynamics; cytoskeleton organization centers; ooplasmic segregation.**

INTRODUCTION

Maternal factors, such as mRNA and proteins, are accumulated in the developing oocyte cytoplasm during oogenesis and play an important role during subsequent development in the control of gene expression (St. Johnston and Nüsslein-Volhard, 1992; Grünert and St. Johnston, 1996; King, 1996). The oocyte also accumulates ribosomes and organelles and in many cases pigment granules and nutrients such as yolk. In most animal species the source of maternal factors and organelles is the oocyte itself that builds up an inventory of these materials during a long maturation period. In some species, however, such as insects and leeches, maternal factors and organelles are mostly produced by nurse cells connected to the maturating oocyte by cytoplasmic bridges (Fernández *et al.*, 1992; Mahajan-Miklos and Cooley, 1994). Maternal factors, organelles, and pigment granules may be scattered across the cytoplasm or congregated in certain regions of the oocyte to form well-defined, specialized cytoplasmic domains. However, the prezygotic distribution pattern of such domains is often dramatically modified in the zygote by ooplasmic segregation. That is the case, for example, in ascidian (Reverberi, 1971; Satoh, 1999), nematode (Bowerman, 1999), and annelid zygotes (Fernández and Olea, 1982; Shimizu, 1982). The new emerging localization pattern of cytoplasmic domains is of great importance for the selective distribution of cytoplasmic domains during cleavage.

The cytoskeleton plays an important role in the transportation, localization, and anchorage of maternal factors and organelles in the zygote of several phyla (reviewed by King, 1996; Glotzer and Ephrussi, 1996; Kemphues and Strome, 1997; Fernández *et al.*, 1998b. see also Astrow *et al.*, 1989; Abraham *et al.*, 1993; Shimizu, 1995; Fernández *et al.*, 1998a). The association of mRNA, ribosomes, and translation factors with the cytoskeleton may lead to the formation of translation complexes that regulate the synthesis of proteins in development (see Bassell *et al.*, 1994a,b; Hamill *et al.*, 1994; Glotzer and Ephrussi, 1996).

[1] To whom correspondence should be addressed at Department of Biology, Faculty of Science, University of Chile, Casilla 653, Santiago, Chile. Fax: 56-2 2712983. E-mail: jfernand@abello.dic.uchile.cl.

0012-1606/00 $35.00

Previous work using the glossiphoniid leech *Theromyzon rude* has shown that its egg and zygote are convenient materials for the study of the role of the cytoskeleton in the establishment of cytoplasmic domains. By the end of the first interphase the egg presents three prominent cytoplasmic domains, rich in organelles and deficient in yolk platelets, along the animal/vegetal axis. One is the centrally located perinuclear plasm that forms in the meiotic egg as result of a microtubule-based transport that leads to organelle accumulation around the sperm-derived centrosome (Fernández *et al.*, 1994). The other two are the polar domains, the animal and vegetal teloplasms, that form in the zygote during the first interphase. The cytoskeleton and organelles first congregate in two polar rings and about a dozen meridional bands. Poleward displacement of the contracting rings and shortening of the meridional bands lead to concentration of the cytoskeleton and organelles at the zygote poles (Fernández and Olea, 1995). This is a three-step segregation process, in which ectoplasmic microtubules and microfilaments are involved (Fernández *et al.*, 1998a). The animal and vegetal teloplasms may be depository of morphogenetic factors engaged in cell fate determination (see Weisblat *et al.*, 1999).

At each cleavage division the perinuclear plasm splits into equal parts that are inherited by the daughter blastomeres. The teloplasms, instead, are funneled along the D blastomere lineage to be finally sequestered into five paired large stem cells called "teloblasts." These cells use the teloplasm in the manufacture of blast cell descendants destined to form ecto- and mesoderm (Fernández, 1980; Fernández and Stent, 1980; Fernández and Olea, 1982).

In this paper we show that the early first interphase leech zygote has a complex cytoskeleton that consists of inner and outer domains. The inner domain, or endoplasmic cytoskeleton, consists of a monaster whose fibers withdraw from the zygote surface toward the end of the early first interphase. The outer domain, or ectoplasmic cytoskeleton, is formed by numerous cytoplasmic asters or cytasters that function as centers of microtubule and microfilament assembly/disassembly. Cytasters exhibit ATP-dependent movements that confer the ectoplasmic cytoskeleton a highly dynamic nature. They accumulate and transport mitochondria, as well as other organelles, across the egg periphery, accomplishing an important role in ooplasmic segregation.

MATERIALS AND METHODS

Eggs or zygotes of the duck leech *Theromyzon trizonare* (formerly confused with *T. rude*, see Davies and Oosthuizen, 1993) were used. Gravid leeches were collected in the ponds of the Golden Gate Park, San Francisco, California, and maintained in the laboratory at room temperature. To delay egg laying, gravid specimens were stored in a climate chamber at 12–14°C. To obtain synchronously developing eggs the ovisacs containing mature eggs were opened in filtered spring water and cultured in the same fluid. Eggs were already fertilized and blocked at metaphase I (Fernández and Olea, 1982). Meiosis concluded at 2:30–3:00 h of development at 20°C, time at which the nascent zygote entered its first interphase.

Preparation of Zygotes for Light and Transmission Electron Microscopy

Zygotes were fixed at room temperature for about 2 h in 2% glutaraldehyde in 0.1 M cacodylate buffer, pH 7.4. To improve cytoskeleton preservation tannic acid (0.15%), Taxol (80 μM), and phalloidin (0.7 μM) were added to the fixative mixture. This procedure increased the number of microtubules and microfilaments detected under fluorescence and electron microscopy. Eggs were rinsed, dehydrated, and embedded in Spurr resin according to Fernández *et al.* (1994).

Preparation of Zygotes for Immunocytochemistry

Staining of microtubules and microfilaments, as well as of centrosomal antigens, was performed in permeabilized-fixed zygotes. For permeabilization mechanically dechorionated eggs were treated for 10 min in PHEM buffer (2 mM $MgCl_2$, 60 mM Pipes, 25 mM Hepes, and 10 mM EGTA; see Schliwa, 1980; Schliwa and van Blerkom, 1981) containing Triton X-100, antiproteases, Taxol (1 μg/ml), and phalloidin (1 μg/ml). After fixation in 4% paraformaldehyde in PBS, zygotes were rinsed and stained for microtubules and microfilaments according to Fernández and Olea (1995). Staining of centrosomal antigens was performed with the following antibodies produced in mouse: anti-centrophilin serum 1:10 in PBS solution (provided by Dr. M. Valdivia), BX-63 anti-centrosome serum 1:2 in PBS solution (provided by Dr. D. Glover), and AH-6 anti-centrosome serum 1:2 in PBS solution (provided by Dr. Biessmann). Rhodamine- or fluorescein-labeled goat anti-mouse IgG was used as a second antibody.

Mitochondria Staining

To trace live mitochondria in first interphase zygotes and to determine their relationships with the cytoskeleton, red (CMTRos) or green mitotracker (Molecular Probes) was used. For this purpose mechanically dechorionated zygotes were loaded for 10 min with mitotracker at a concentration of 45 μg/ml in spring water. After several rinses in spring water zygotes were whole mounted between two coverslips. For double labeling, mitotracker was loaded in zygotes preinjected with either labeled tubulin or actin.

Fluorescence Video Microscopy and Image Processing

Live eggs microinjected with labeled probes or loaded with mitotracker were studied in an Axiovert 135 inverted Zeiss fluorescence microscope equipped with either a Sony CCD video camera (Model DXC-C1) or a Hamamatsu chilled CCD camera (Model C5985 with a Photoshop plug-in module). Images captured with the Sony camera were digitized by a LG-3 Scientific frame grabber (PCl version, Scion Corporation, Frederick, MD). Image analysis was performed on a Power Macintosh 8500 computer using the public domain NIH program (written by W. Rasband at the U.S. National Institutes of Health). Images were frame averaged and contrast enhanced, the gray level was properly adjusted, and in some cases pseudocolor was assigned. Images captured with the

Hamamatsu camera were processed by either the Photoshop software or the NIH program. Time-lapse images were captured every 2–30 min and the results were analyzed in animated sequences or multiple montages.

Preparation of Labeled Tubulin

Tubulin was purified from a chicken brain homogenate according to the method of Weisenberg *et al.* (1968) as modified by Monasterio and Timasheff (1987). SDS–PAGE of the purified tubulin showed a single band at 55 kDa. Optical density reading at 276 nm indicated a tubulin concentration of 30–40 mg/ml. Tubulin was conjugated to the following fluorophores according to Hyman *et al.* (1991): 5-(and 6)-Carboxyfluorescein succinimidyl ester and 5-(and 6)-carboxytetramethylrhodamine succinimidyl ester (Molecular Probes). Replacement of the conjugation buffer for the injection buffer was achieved by centrifugation at 30 psi for 20 min. The fluorophore/tubulin dimer ratio was 2:1. Labeled tubulin was aliquoted and stored at −20°C.

Preparation of Labeled Actin

Actin was purified from acetone powder obtained from chicken breast according to Pardee and Spudish (1982). SDS–PAGE of the purified G-actin gave a single band at 45 kDa. Conjugation of F-actin to the fluorophore was done according to Bearer (1992). Both carboxyfluorescein and carboxytetramethylrhodamine succinimidyl esters (Molecular Probes) were used. The fluorophore/actin monomer ratio was 3:1. After centrifugation the actin conjugate was stored at 4°C in depolymerizing buffer. Before use the depolymerizing buffer was replaced by the acetate injection buffer through several centrifugations at 13,000 rpm using an Amicon tube.

Microinjection. Labeled tubulin or labeled actin, Taxol (paclitaxel, Molecular Probes), and AMP–PNP (5′adenylimidodiphosphate, Calbiochem) were pressure injected under a dissecting microscope. The egg is 700–750 μm in diameter and its volume was estimated to be approximately 200 nl. Single or double injections were always placed at the equatorial region of the egg or zygote and the amount of fluid microinjected varied between 0.5 and 4 nl.

Tubulin and actin. To determine the assembly dynamics of the ectoplasmic cytoskeleton, chicken tubulin or actin, labeled with rhodamine or fluorescein, was microinjected at meiosis I (about 30 min of development), meiosis II (about 2 h of development), or during early first interphase (2:30–3:00 to 3:30–4:00 h of development). Tagged tubulin (3.5 mg/ml) was dissolved in glutamate injection buffer (0.5 mM glutamic acid, 50 mM potassium glutamate, 0.5 mM $MgCl_2$, pH 6.5; see Hyman *et al.,* 1991), whereas labeled actin (3.7 mg/ml) was dissolved in acetate buffer (2 mM Tris acetate, pH 7.0, 0.2 mM ATP, 0.05 mM $MgCl_2$; see Hird, 1996). Microinjection of 0.5–1 nl of labeled tubulin or actin gave a final intracellular concentration of 1.7–3.5 ng. Zygotes that were microinjected with either of the probes, or coinjected with the two probes, were studied by time-lapse video fluorescence. To determine whether fluorescence detected in zygotes was due to incorporation of the labeled probe into microtubules or microfilaments or to the accumulation of labeled subunits, microinjected zygotes were examined under the fluorescence microscope during and after the permeabilization procedure.

Taxol. The effect of Taxol on microtubule polymerization and dynamics was assessed in zygotes preinjected with labeled tubulin. Working solutions of 1, 2, 5, 15, 25, 35, and 50 mM Taxol, diluted in DMSO, were used. Microinjection of 0.5 nl of the working solution gave the following approximate intracellular concentrations of Taxol: 2.5, 5, 12.5, 37.5, 62.5, 87.5, and 125 μM, respectively. In all cases the final intracellular concentration of DMSO was about 0.25%.

AMP–PNP. To determine whether cytaster movement was an ATP-dependent process, zygotes preinjected with labeled tubulin or actin received a second microinjection of the ATP analog AMP–PNP. Working solutions of 0.05, 0.24, and 0.47 M AMP–PNP in glutamate injection buffer were prepared. Each zygote received 4 nl of the working solution to reach intracellular concentrations of approximately 10, 50, and 100 mM.

RESULTS

The observations were made during early first interphase that extends between completion of the second meiotic division and initiation of major furrowing activity. Major furrowing activity is marked by the appearance of the animal polar ring. At 20°C the early first interphase is completed in about 1 h (Fernández *et al.*, 1998a).

The Cytoskeleton of the Late Meiotic Egg and Early First Interphase Zygote

Examination of sectioned late meiotic eggs or early first interphase zygotes stained for α-tubulin reveal that their cytoskeleton consists of internal and external microtubule domains. The internal, or endoplasmic, domain corresponds to a monaster that consists of a centrally located microtubule nucleation center and numerous bundles of microtubules that extend radially to the zygote periphery (Figs. 1A and 1B). The monaster fibers enter into the ectoplasm but it is not clear how far their microtubules extend. The external, or ectoplasmic, microtubule domain appears as a thick scalloped layer, 7–10 μm thick, formed by rounded bundles of microtubules often arranged into semicircular bodies (Fig. 1C). Toward the end of the early first interphase, the distal segment of the monaster fibers loses contact with the zygote periphery and becomes highly distorted and a nonfluorescent zone appears beneath the ectoplasm. Concomitantly the ectoplasmic microtubule domain becomes thinner (about 5 μm thick) and adopts a beaded appearance (Figs. 1D and 1E) similar to that seen in the early meiotic egg (Fig. 1F), at a time before it has formed a monaster (see Discussion). As shown in Fig. 1G, the beaded appearance of the zygote ectoplasm is due to numerous foci of microtubules that can be visualized across the surface of whole-mounted zygotes stained for tubulin. Similar foci of actin filaments are seen in whole-mounted or sectioned zygotes stained with labeled phalloidin (Fig. 1H).

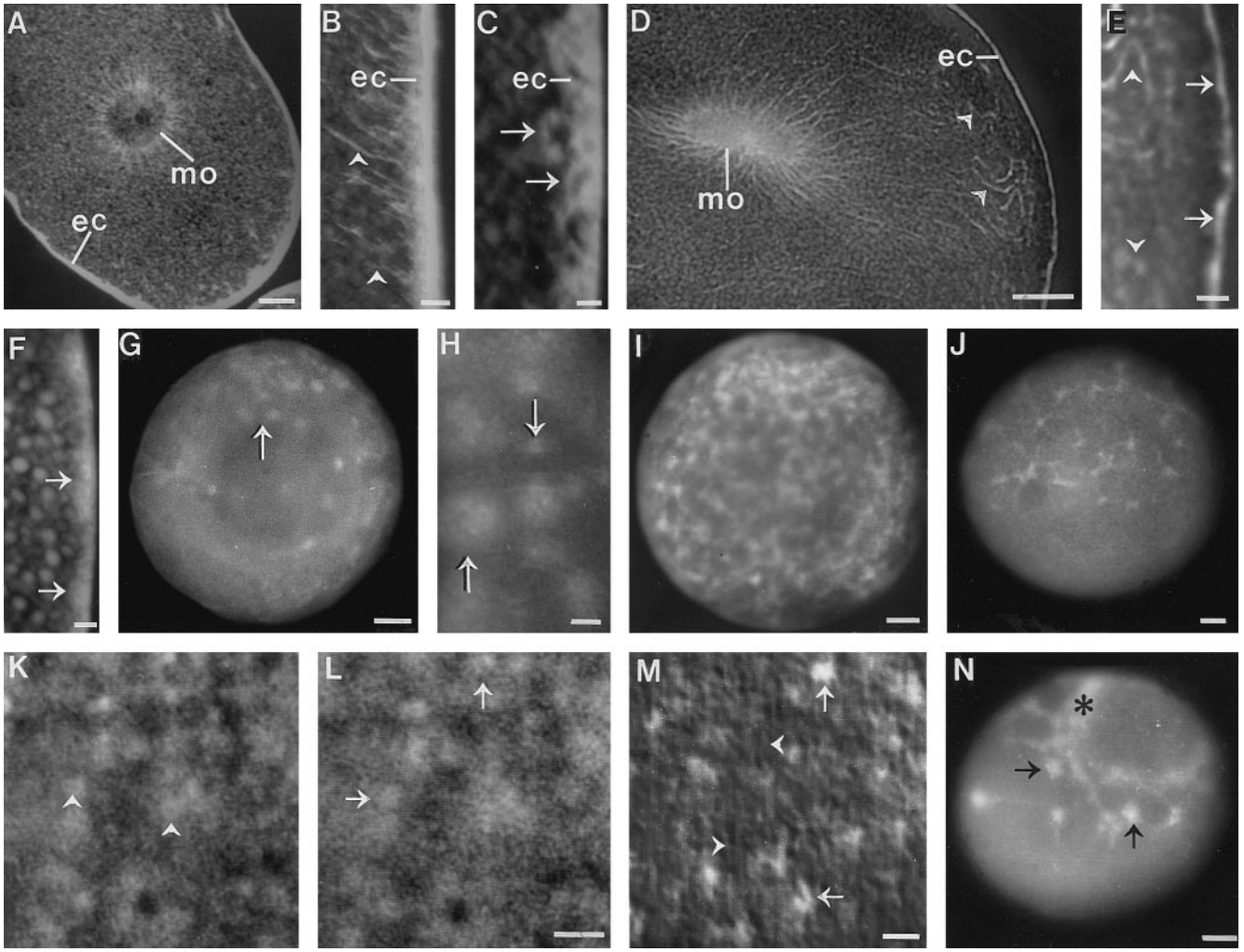

FIG. 1. Organization of the endoplasmic and ectoplasmic cytoskeleton domains in early first interphase zygotes studied by immunofluorescence (A–H) and after microinjection of labeled tubulin or actin (I–N). (A) Cross-section of a zygote embedded in glycol methacrylate and stained for α-tubulin that shows the monaster (mo) and the ectoplasmic domain of microtubules (ec). (B) Periphery of a similar zygote showing monaster fibers (arrowheads) entering the ectoplasm (ec). (C) Periphery of the same zygote showing thick bundles of microtubules, presumably monaster fibers, scattered across the ectoplasm (ec). Notice that microtubule bundles tend to be arranged in semicircular structures (arrows). (D) Cross-section of a zygote embedded in plastic and stained for β-tubulin that shows the center of the monaster (mo) and its fibers that have lost connection with the ectoplasm (ec). Interrupted monaster fibers become highly distorted (arrowheads). (E) Periphery of the same zygote showing the interrupted monaster fibers (arrowheads) and the beaded appearance (arrows) of the ectoplasmic microtubule domain. Notice the microtubule-free zone underlying the ectoplasm. (F) Section across the periphery of an early meiotic egg embedded in plastic and stained for α-tubulin. Notice the beaded appearance (arrows) of its ectoplasmic domain of microtubules. (G) Animal pole view of a whole-mounted zygote stained for α-tubulin that shows foci of microtubules (arrow) scattered throughout the ectoplasm. (H) Surface view of a whole-mounted zygote stained with rhodamine–phalloidin that shows several foci of actin filaments (arrows). (I) Lateral view of a live zygote microinjected with rhodamine–tubulin during the meiotic period that shows accumulation of the probe in a peripheral network of fluorescent foci. (J) Similar view of another live zygote microinjected with rhodamine–actin that shows accumulation of the probe in a similar network of fluorescent foci. (K and L) Confocal sections of a live rhodamine–tubulin microinjected egg taken at 3 and 5 μm of depth, respectively, that show tiny star-shaped fluorescent foci (arrows), some with a nonfluorescent center (arrow heads), whose processes interdigitate with one another. (M) Surface view of a live zygote microinjected with rhodamine–tubulin. This electronically shadowed image shows irregularly shaped fluorescent foci (arrows) whose processes interdigitate and form thick fibers (arrowheads). (N) Permeabilized zygote previously microinjected with rhodamine–tubulin. Notice that fluorescence persists in ectoplasmic foci (arrows) as well as in the animal polar ring (asterisk). Hence these regions incorporated microinjected tubulin into microtubules. Bars, 100 μm (G, H, I, and N); 80 μm (J); 30 μm (A and D); 10 μm (B, L, and M); 6 μm (C, E, and F).

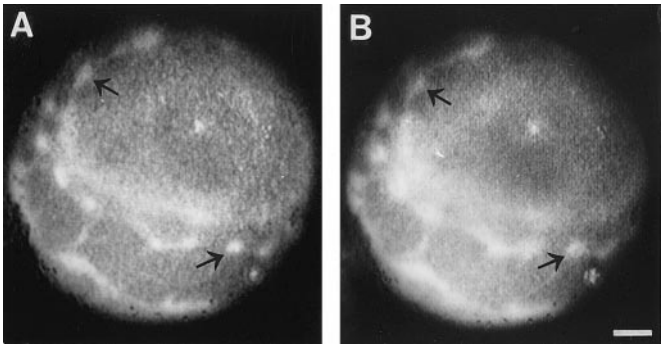

FIG. 2. Whole-mounted live first interphase zygote microinjected with a mixture of rhodamine–tubulin and fluorescein–actin during the meiotic period. Notice colocalization of microtubules (A) and actin filaments (B). Arrows point to cytasters. The fuzzy appearance of the actin network is due to the zygote autofluorescence. Bar, 100 μm.

We are not yet certain, however, whether an endoplasmic actin cytoskeleton also exists.

Accumulation of Microinjected Labeled Tubulin and Actin in Discrete Bodies Distributed across the Ectoplasm

Eggs or zygotes that were microinjected with either labeled tubulin or labeled actin, during the meiotic or interphase period, and examined toward the end of early first interphase reveal the presence of numerous irregularly shaped fluorescent bodies throughout the egg periphery (Figs. 1I and 1J). The size and brightness of these bodies increase during early interphase, in part due to their fusion. When first seen they are 5–20 μm in diameter reaching up to 70 μm by the end of the early first interphase. Optical sections of tubulin-labeled zygotes examined under the confocal microscope show that the fluorescent bodies are star-shaped structures that can include a central unlabeled region (Figs. 1K and 1L). Fine filaments radiating out from the fluorescent bodies interdigitate with one another forming thicker filaments. These are well shown in electronically shadowed images like the one in Fig. 1M. Examination of permeabilized zygotes microinjected with either marked tubulin or actin show that the fluorescent bodies remain in place after a procedure that is intended to extract soluble components such as monomeric tubulin and actin. The fact that permeabilized fluorescence bodies lose brightness indicates that both polymerized and unpolymerized probes are sequestered in their interior (Fig. 1N).

The sizes, structure, and distribution of the fluorescent bodies are similar to those of the fluorescent foci detected by immunocytochemistry. Furthermore, coinjection of labeled tubulin and actin shows colocalization of both probes (Figs. 2A and 2B). These results indicate that the fluorescent foci and the fluorescent bodies are the same thing: centers of microtubule and microfilament accumulation. These centers have similarities with cytoplasmic asters described in other cells (see Discussion), and for this reason they are called cytasters.

Time-Lapse Video Microscopy of Moving Cytasters

Time-lapse video tracing of cytasters labeled with either fluorescent tubulin or/and actin show that they could move in an orderly manner at speeds of 0.5–2.5 μm/min (Figs. 3A–3G). This speed was estimated by computing time vs distance between neighboring cytasters. As shown in Figs. 4A–4D, cytaster movement begins to be affected by intracellular concentrations of 10 mM AMP–PNP. At this concentration cytaster movement is slowed down or interrupted. At higher concentrations the zygotes die. Colliding cytasters fuse and form larger cytoskeletal bodies (Figs. 4E–4F).

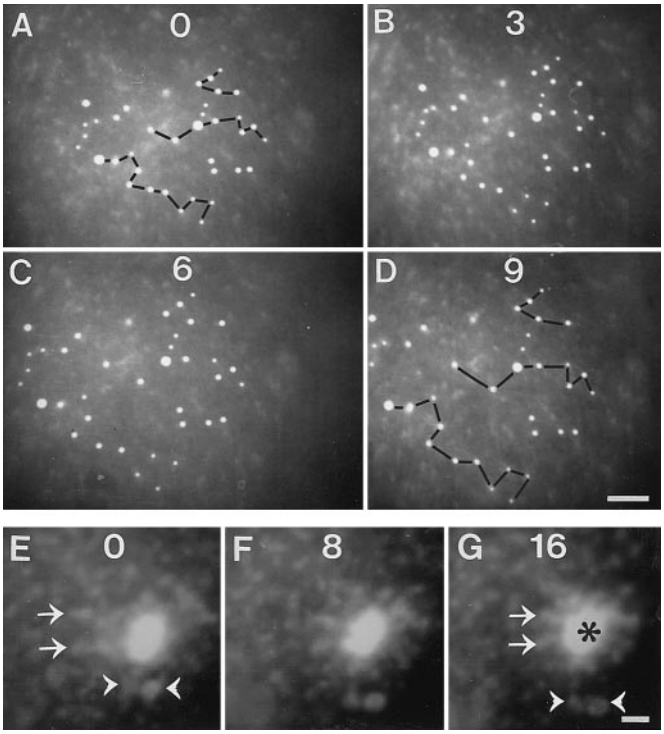

FIG. 3. Movement of microtubule and microfilament cytasters determined by time-lapse video imaging of microinjected early first interphase zygotes. (A–D) Montage of a rhodamine–tubulin-microinjected zygote that shows movement of microtubule cytasters during a period of 9 min. To facilitate tracing of the cytasters some of them are marked with white dots of different size linked by black bars (Compare 3A with 3D). Notice that marked cytasters are moving away from one another. (E–G) Montage of a rhodamine–actin-microinjected zygote that shows movement of actin cytasters during a period of 16 min. Cytasters converging (arrows) into a labeled region of the zygote (asterisk) or diverging from it (arrowheads) are shown. Bars, 50 μm (D); 30 μm (G).

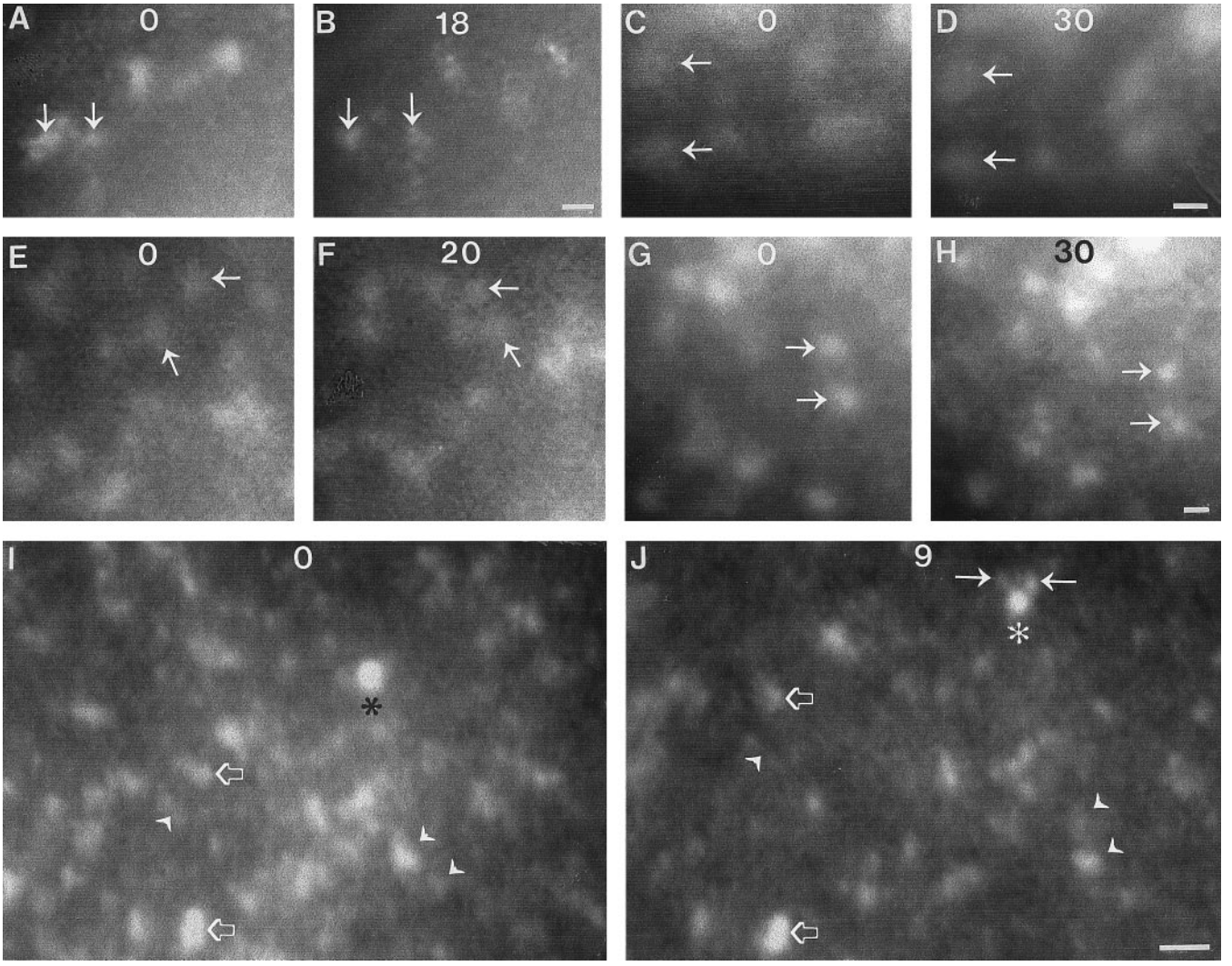

FIG. 4. Detention of cytaster movement and variation of their fluorescence in early first interphase zygotes microinjected with labeled tubulin. (A–D) Montage that shows the effect of different concentrations of AMP–PNP on cytasters that are moving away from one another (arrows). A 5 mM intracellular concentration of the analog does not affect cytaster movement (A and B, time 18 min), whereas a 10 mM intracellular concentration stops cytaster movement (C and D, time 30 min). (E–H) Montage that shows the effect of different concentrations of Taxol on cytasters that are approaching to one another (arrows). A 37.5 μM intracellular concentration of the drug does not affect cytaster movement (E and F, time 20 min). Notice that cytasters fuse with one another to form larger cytoskeletal bodies. A 125 μM intracellular concentration of Taxol stops cytaster movement (G and H, time 30 min). (I and J) Montage that shows fluctuations in cytaster brightness (compare arrowheads) with time (9 min). Most cytasters are seen moving away from one another (compare open arrows) and in some regions (asterisks) they seem to be forming *de novo* (arrows). Bars, 30 μm (B); 20 μm (D); 10 μm (H, J).

Figures 4E–4H show the effect of microinjected Taxol on cytaster movement. Low intracellular concentrations of the drug (2.5–37.5 μM) do not affect or slow down (20–50%) cytaster movement, whereas higher intracellular concentrations (starting with 62.5 μM) block their movement.

In some regions cytasters display synchronized divergent or convergent movements. Furthermore, time-lapse tracing of individual microtubule cytasters shows that their movement may be accompanied by changes in fluorescence emission. In some cases cytasters seem to disappear from scene and reappear after a few minutes (Figs. 4I and 4J).

Cytasters Are Centers of Microtubule and Microfilament Nucleation during Early First Interphase

To investigate the possibility that cytasters are centers of microtubule and microfilament nucleation we carried out

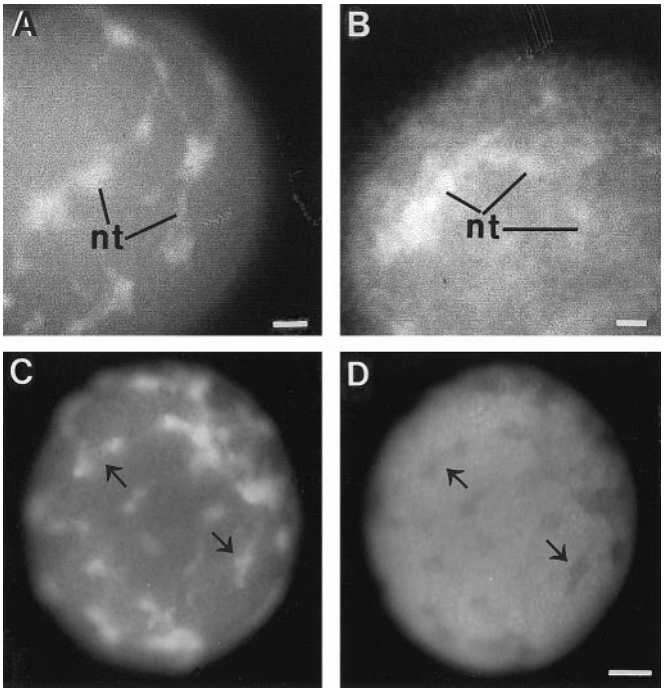

FIG. 5. Whole-mounted live early first interphase zygotes that show incorporation of labeled actin (A) and labeled tubulin (B) in a cytaster network (nt) after short pulses of the microinjected probe, and the colocalization (arrows) of a network of microtubule cytasters (C) with a network of furrows (D) sculptured on the zygote surface. The latter zygote was viewed with the fluorescein filter. Bars, 100 μm (D). 50 μm (A, B).

two types of experiment. First, zygotes were examined shortly after receiving brief pulses of labeled tubulin and/or labeled actin during different periods of the early and mid first interphase. It was found that cytasters always incorporate the probes, indicating that during those periods they are constantly functioning as microtubule and microfilament organization centers (Figs. 5A and 5B). Second, double injection of labeled tubulin and Taxol increases cytaster fluorescence because more microtubules are being assembled. It might be argued that expansion of the tubulin and/or actin pool in microinjected zygotes induces cytaster formation. However, there is an important reason for rejecting this possibility: microtubule and actin cytasters are seen in immunostained eggs and zygotes that have not been exposed to additional exogenous tubulin or actin.

Toward the end of the early first interphase, the position of cytasters is marked by depressions of the zygote surface (Figs. 5C and 5D). These depressions are probably already present at an earlier stage, but due to their small size remain undetected under the fluorescence microscope. This conjecture is supported by light and electron microscopic studies presented below.

Immunocytochemical Demonstration That the Network of Cytasters Contains Centrosomal Antigens

Since cytasters function as microtubule-organizing centers it was important to determine whether they contained centrosomal antigens. To this end zygotes that have completed the early first interphase, marked by the formation of the animal polar ring, were immunostained for centrosomal proteins. Due to the moderate signal emitted by the stained centrosomes and the strong zygote autofluorescence it was not possible to double stain cytasters to show colocalization of centrosomal proteins and microtubules. To test the antibodies specificity, zygotes that have already assembled the cleavage spindle were also immunostained for centrosomal antigens. Observations show that the network of cytasters, together with the animal polar ring (Figs. 6A–6C), and the cleavage spindle poles (Figs. 6D, 6E, and 6G) stain with the following antisera: anti-centrophilin, anti-BX-63, and anti-AH-6. The position and large size of the cleavage spindle centrosomes can be appreciated in Fig. 6F that corresponds to a dividing zygote stained for β-tubulin (compare with Fig. 6D).

Cytasters as Sites of Organelle Accumulation

Fluorescent bodies, similar in size and motility to the cytasters detected after injection of labeled tubulin or actin, are also seen throughout the ectoplasm of early first interphase zygotes previously loaded with mitotracker (Fig. 7A). Furthermore, the clusters of mitochondria become interconnected forming a network (Fig. 7B), whose size and brightness gradually increase (Figs. 7C–7G). Eggs microinjected with fluorescein-labeled tubulin, and then loaded with red mitotracker, show that marked mitochondria colocalize with microtubule cytasters and move together (Figs. 7H and 7I).

To corroborate these results and to determine whether other organelles also accumulate in cytasters during early first interphase, zygotes were examined under light and electron microscopy. Early cytasters are identified as slightly depressed regions of the zygote surface having thickened ectoplasm (Figs. 8A and 8B). The ectoplasm has an outer microfilament-rich cortex and an inner subcortex with microtubules, granular material, and diverse organelles in moderate amounts. Microtubules are found near the cortex and close to mitochondria, which constitute the most common organelle of the cytaster. Microfilaments could not be unambiguously identified in the subcortex (Figs. 8C and 8D). Comparison of cytasters throughout the first interphase shows that their development is marked by deeper depressions of the zygote surface and increased thickness of their ectoplasm (Fig. 9A). The cytaster cortex does not seem to change, but its subcortex shows greater accumulation of granules and organelles (Figs. 9B–9D). Accumulation of mitochondria is particularly striking. They appear as rounded, elongated, or figure-of-eight bodies, suggesting that the organelle is actively proliferating

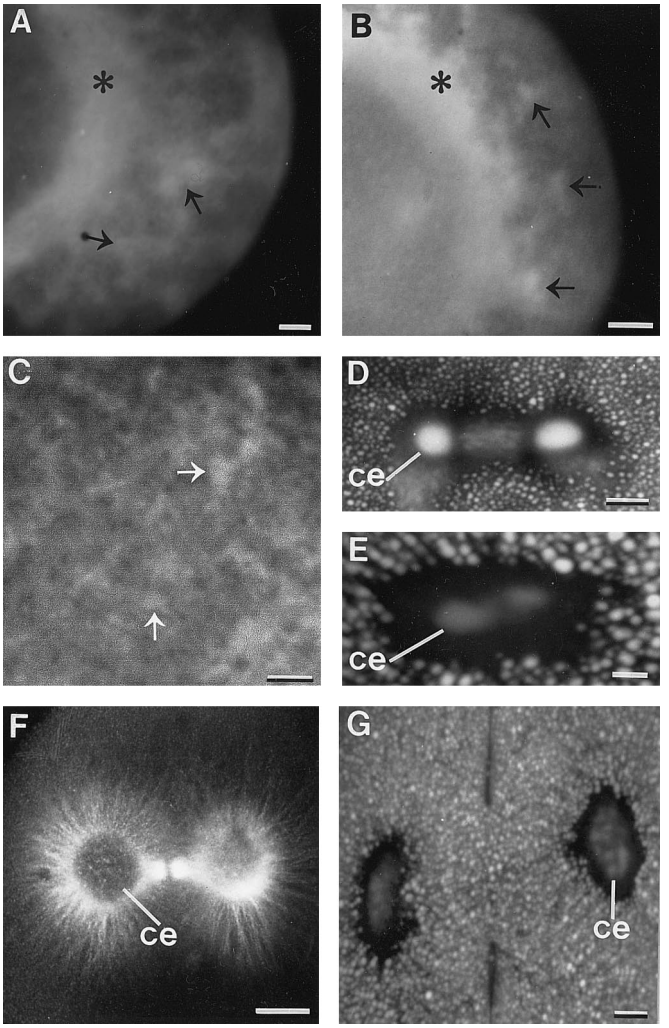

FIG. 6. Immunofluorescence detection of centrosomal antigens in the network of cytasters of whole-mounted early first interphase zygotes (A–C) and in the centrosomes of sectioned first cleavage spindles (D, E, and G). (A) Zygote stained for the AH-6 antigen that is present in the animal polar ring (asterisk) and in cytasters (arrows). (B) Similar zygote stained for centrophilin showing a similar distribution of the antigen in the polar ring (asterisk) and cytasters (arrows). (C) Higher magnification of the network of cytasters (arrows) stained for the AH-6 antigen. (D) The centrosomes (ce) of the cleavage spindle are strongly stained for centrophilin, while the spindle fibers are lightly stained. (E) Only the spindle centrosomes (ce) are seen stained with the AH-6 antibody. (F) Whole-mounted mitotic zygote showing the first cleavage spindle stained for α-tubulin. Notice the large size of the centrosomes (ce). (G) Cleaving zygote that shows the centrosomes (ce) of the first two blastomeres stained for centrophilin. Bars, 30 μm (A, B, D, and F); 10 μm (C, E, and G).

(see also Fernández *et al.*, 1998a). There are numerous membranous profiles that correspond to a combination of vesicle and branched tubular structures, some studded with ribosomes, that undoubtedly correspond to a mixture of smooth and rough endoplasmic reticulum. Microfilaments could not be visualized across the subcortex.

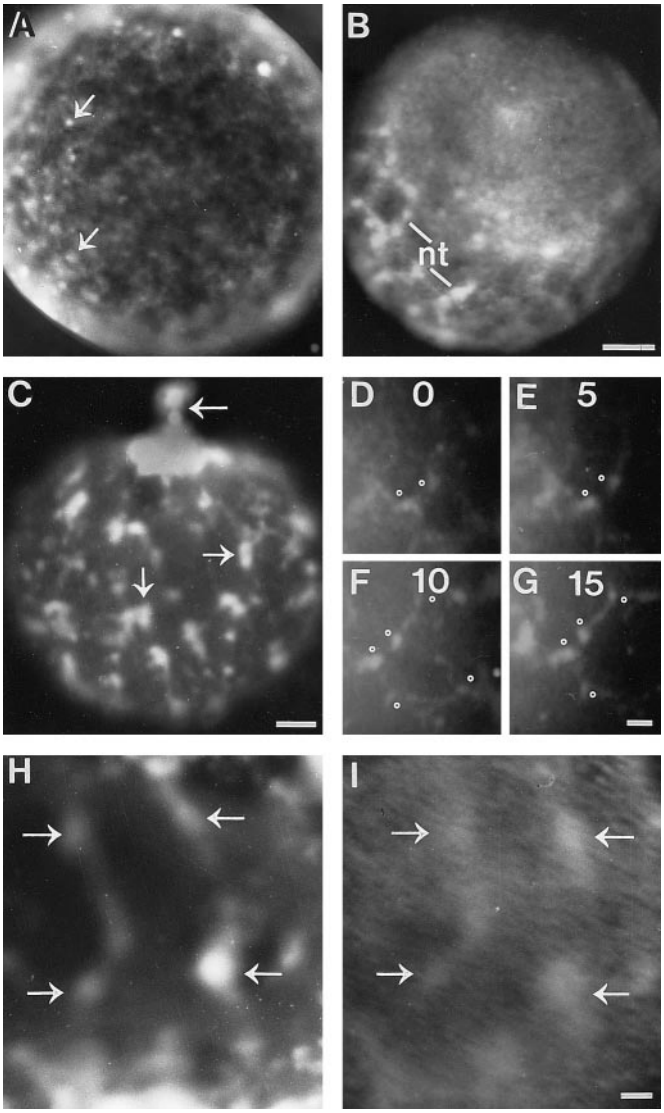

FIG. 7. Whole-mounted live first interphase zygotes loaded with red mitotracker. (A) Small bright spots (arrows) scattered across the zygote surface correspond to sites of mitochondria accumulation and closely resemble the size and distribution of cytasters. (B) Same zygote 20 min later showing that mitochondrial clusters are larger and brighter and form a network (nt). (C) As with cytasters, mitochondrial clusters have fused into larger bodies arrows. The two pole cells are shown (top arrow). (D–G) Montage that shows formation of a network of mitochondrial clusters during a 15-min period. The small white circles serve as reference points to follow the mitochondrial clusters. (H and I) Colocalization of mitochondrial clusters (H) and microtubule cytasters (I), assembled from fluorescein-labeled tubulin. Arrows mark the same regions of the zygote. Bars, 100 μm (B, C); 50 μm (I); 30 μm (G).

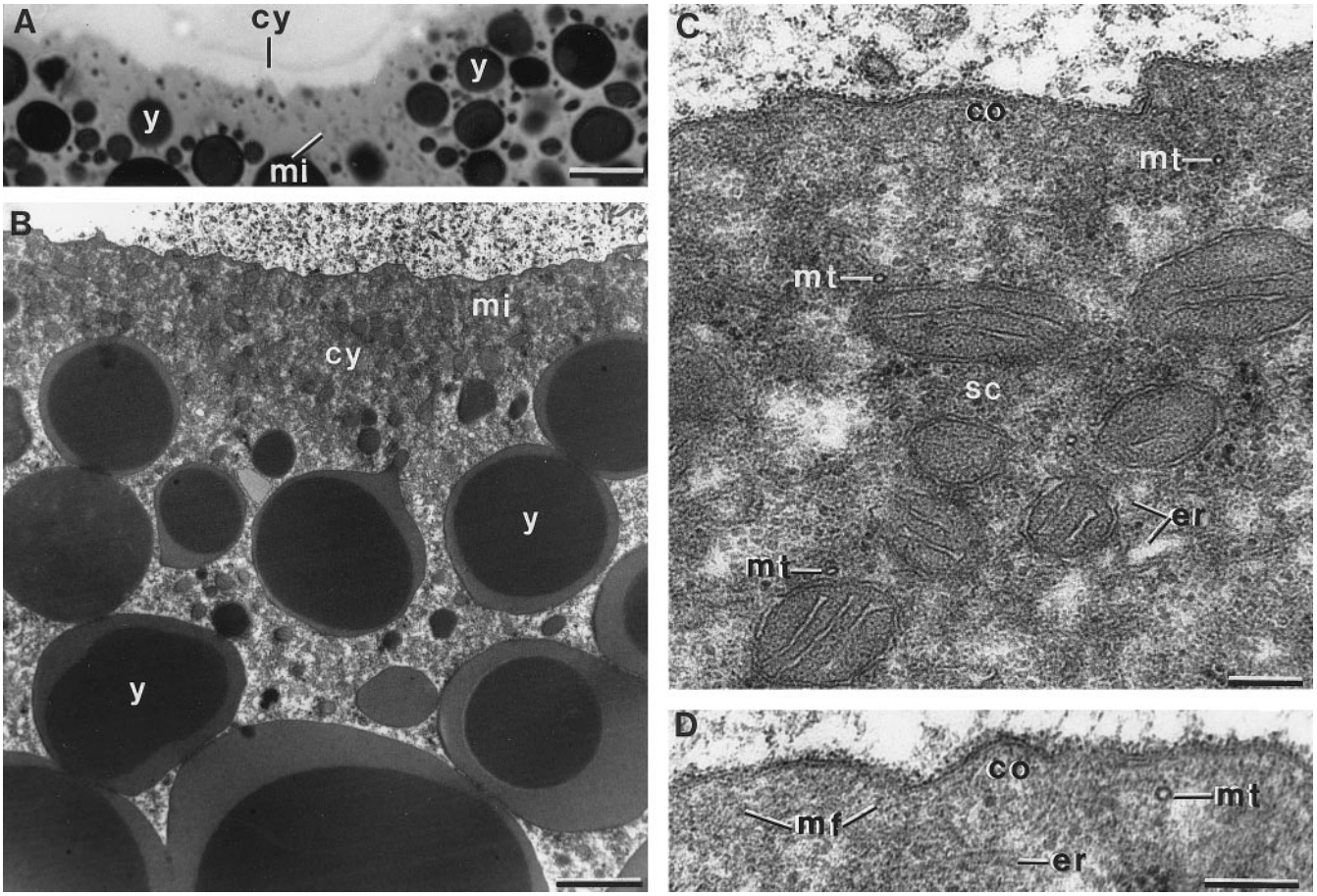

FIG. 8. Light and electron micrographs showing the structure of the cytasters during the second half of the early first interphase. (A and B) Cytasters (cy) appear as regions of slightly depressed and thickened ectoplasm that enclose a moderate number of organelles, particularly mitochondria (mi). Yolk platelets (y) are abundant in the endoplasm. (C and D) At higher magnification one detects the cortical (co) and subcortical (sc) regions of the cytaster. The microfilament (mf)-rich cortex surmounts a subcortex that has numerous microtubules (mt) and a moderate number of granules and organelles such as mitochondria and endoplasmic reticulum (er). Microtubules are commonly seen near mitochondria and the cortex. Bars, 7 μm (A); 2 μm (B); 0.2 μm (C, D).

DISCUSSION

The Two Cytoskeletal Domains of the Early First Interphase Zygote

A striking feature of the first interphase leech zygote is the complexity of its cytoskeleton that comprises two different domains. The endoplasmic or inner domain corresponds to the first interphase monaster whose radially running microtubules are nucleated by the sperm-derived centrosome (Fernández *et al.*, 1994). The leech zygote monaster is thus similar in origin and structure to the monaster found in the zygote of other species, such as the sea urchin (Harris, 1981) and the frog (Gard *et al.*, 1995).

By contrast, the ectoplasmic or outer domain of microtubules of the early first interphase leech zygote, being formed by interconnected foci or cytasters, represent a peculiar case encountered in the normal zygote of very few species. Interestingly enough, the zygote network of microtubule cytasters becomes visible by the time monaster fibers interrupt their connections with the ectoplasm. However, cytasters can be visualized before in the early meiotic egg, whose monaster has not yet been assembled (see Fernández *et al.*, 1994). These results suggest that the endoplasmic and ectoplasmic microtubule domains are separate systems that probably form independently. It is presumed that cytasters arise from discrete sites of accumulation of centrosomal antigens capable of nucleating microtubules across the ectoplasm.

Both domains of microtubules in the leech egg and zygote appear involved in organelle translocation. However, their different organization suggests that they do similar tasks in different ways. The endoplasmic microtubules seem to

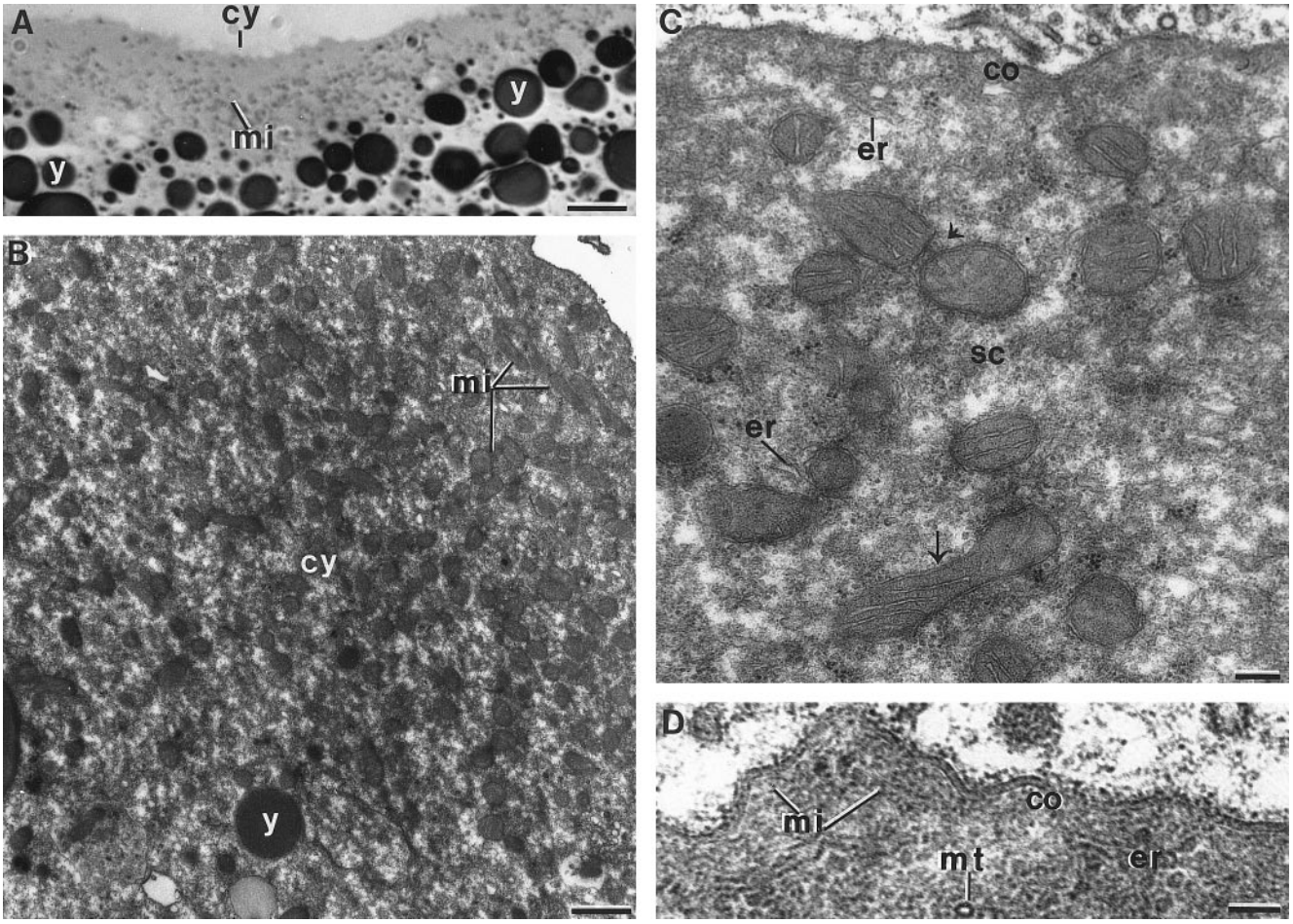

FIG. 9. Light and electron micrographs showing the structure of the cytasters by the end of the early first interphase. (A and B) Cytasters (cy) appear as much thicker regions of the ectoplasm that enclose numerous organelles, particularly mitochondria (mi). Large yolk platelets (y) mark the ectoplasm inner boundary. (C and D) At higher magnification one verifies that the structure of the cortex (co) does not seem to have changed much, including numerous microfilaments (mf). The subcortex (sc) shows elongated mitochondria that will probably divide (arrow) or have just come apart (arrow head). Numerous granules and profiles of endoplasmic reticulum (er) are seen. As in less-developed cytasters, microtubules are found near mitochondria and the cortex. Bars, 8 μm (A); 1 μm (B); 0.2 μm (C); 0.1 μm (D).

provide radially arranged routes for organelles to flow centripetally in the (+) → (−) direction or centrifugally in the (−) → (+) direction. Thus, centripetal organelle translocation is probably involved in the formation of the perinuclear plasm domain at the egg center (Fernández *et al.*, 1994), whereas the centrifugal organelle translocation is probably responsible for the accumulation of numerous organelles in the zygote ectoplasm (Fernández *et al.*, 1998a). As shown in this paper, ectoplasmic microtubules organized in cytasters seem to function differently. They behave as carriers, rather than rails, for bulk transportation of organelles across the ectoplasm.

An ectoplasmic cytoskeleton made of mobile nucleation centers would facilitate reiterative episodes of cytoskeleton reorganization, and this is what actually happens in the leech zygote (Fernández and Olea, 1995). Late meiotic and first interphase *Tubifex* eggs also form inner and outer cytoskeleton domains, but in this case they are made of actin instead of a combination of actin filaments and microtubules. Interestingly, the outer actin filaments are also arranged in foci (Shimizu, 1984, 1997).

Interphase Cytasters as Centers of Microtubule and Microfilament Assembly/Disassembly

Evidence presented in this paper indicates that cytasters are centers for the nucleation of polymerization of both microtubules and microfilaments. However, structures so far reported in the literature as cytasters nucleate microtubules only. It is the case, for example, of cytasters in insect parthenogenetic eggs (Riparbelli *et al.*, 1998) and mouse oocytes (Maro *et al*, 1985; Schatten *et al.*, 1985). Foci of

actin nucleation have been reported in *Tubifex* eggs (Shimizu, 1997) and budding yeast (Adams and Pringle, 1984; Kilmartin and Adams, 1984; Mulholland *et al.*, 1994; Li *et al.*, 1995; Winter *et al.*, 1997; Lechler and Li, 1997). These actin foci have motility and bear some similarities with leech cytasters. For this reason they may be considered actin cytasters. Hence, cytasters can be built upon microtubules, microfilaments, or a mixture of both. In some cells microtubule cytasters do not form spontaneously but can be induced to form by Taxol a drug that is known to favor microtubule nucleation by lowering the critical tubulin concentration (De Brabander *et al.*, 1981). One good example of this is the Taxol-induced formation of cytasters in sea urchin oocytes (Harris and Clason, 1992).

Leech zygotes resemble *Xenopus* eggs (Gard *et al.*, 1990; Buendia *et al.*, 1990) and mouse oocytes (Maro *et al.*, 1985) in that their cytasters include centrosomal material and hence constitute classical centers for the initiation of microtubule polymerization. However the nondiscrete distribution of centrosomal antigens in leech cytasters generates some confusion. It is possible that during cytaster collision and coalescence their centers, presumably containing a centrosome, overlap with their processes lacking centrosomal proteins. This situation might yield a diffuse distribution of the antigens. However, diffuse distribution of centrosomal antigens, such as γ-tubulin, is reported to occur throughout the extensive cytoplasm of the giant fresh water ameba *Reticulomyxa filosa* (Kube-Granderath and Schliwa, 1997). Moreover, centrosomal antigens can be found in the mitotic spindle poles and also diffusely distributed on intermediate filaments (Buendia *et al.*, 1990).

Since the cytasters of the early first interphase leech zygote assemble microtubules and microfilaments continuously, they must also be depolymerizing their cytoskeleton continuously. Hence, cytasters can be considered centers of cytoskeleton assembly/disassembly.

The Dependence of Cytasters Motility on both Microtubules and Microfilaments

The rate at which cytasters move during early first interphase is similar to that at which chromosomes move along the spindle in *Xenopus* oocyte extracts or in somatic cells (Desai *et al.*, 1998) and to the speed at which microtubules and microfilaments backflow in lamellipodia of moving cells (Waterman-Storer and Salmon, 1997). Yeast actin patches also move in the plane of the cortex but at much higher speed (Doyle and Boekstein, 1996; Waddle *et al.*, 1996; Winter *et al.*, 1997). Movement of yeast actin patches as well as leech cytasters might facilitate programmed changes in cytoskeleton organization. Thus, formation of contraction rings relies on the orderly accumulation of actin patches in yeast (Machesky, 1998) and of cytasters in leech zygotes (unpublished observations).

Cytaster movement is an ATP-dependent process since it is slowed and finally stopped by AMP–PNP in a dose-dependent manner. Similar results were obtained by Desai *et al.* (1998) in their study of poleward microtubule flux in *Xenopus* extract spindles. An important question to answer is how ATP energy is utilized during cytaster movement. The fact that high concentrations of Taxol paralyze cytasters suggests that their movement would rely on sliding of microtubules subjected to polymerization/depolymerization. However, this might be only part of the explanation since the action of colchicine and cytochalasin B (see Fernández *et al.*, 1998a), indicate that cytaster movement probably depends on both microtubules and microfilaments. The results of Taxol treatment may be interpreted as showing that the drug produces "freezing" of a microtubule array, which in turn immobilizes the colocalized actin lattice. Hence, ATP energy is probably consumed in both microtubule and actin sliding using appropriate motors and regulatory proteins (Yeh *et al.*, 1995; Carminati and Stearns, 1997; Cottingham and Hoyt, 1997). Due to the superficial position of cytasters, the possibility cannot be dismissed that their movement may also depend on the interaction of its cytoskeletal components with cortical sites, a situation that occurs during centrosome movement and spindle positioning in mitotic cells (Karsenti *et al.*, 1996). Finally, the fact that the cytaster cytoskeleton is constantly assembling/disassembling, polymerization/depolymerization of microtubules and microfilaments may also contribute to cytaster movement (reviewed by Inoué and Salmon, 1995; Mitchison and Cramer, 1996; Svitnika *et al.*, 1997).

Cytasters as Sites for Organelle Accumulation and Vehicles for Bulk Transportation of Organelles

There are several reports in the literature indicating that microtubule aster configurations are very important for concentrating cytoplasmic components such as centrosomal material (Dirksen, 1961; Kallenbach, 1985; Buendia *et al.*, 1990; Harris and Clason, 1992) or mitochondria (Van Blerkom, 1991; Pereira *et al.*, 1997). The last authors have even proposed that an aster configuration, such as that of the spindle, may be required to properly segregate mitochondria during cell division. On the other hand, interaction between mitochondria and other organelles with the actin cytoskeleton is known to take place in budding yeast (Boldogh *et al.*, 1998), squid axoplasm (Bearer *et al.*, 1993), ascidian and *Tubifex* eggs (Jeffery, 1995; Shimizu, 1995), and in many cells as part of the intracellular organelle targeting process. Therefore, the combined microtubule/microfilament cytaster appears as a suitable device to collect and transport numerous mitochondria and other organelles throughout the leech zygote.

Increasing accumulation of mitochondria throughout the ectoplasm is the result of two processes: a microtubule-based transport of mitochondria from the neighbor endoplasm and replication of the organelle (Fernández *et al.*, 1998a). When mitochondria reach the ectoplasm they must be transferred from the monaster fibers to the cytasters. This requires that the two type of microtubules be interconnected, and this may be achieved by overlapping or perhaps via microfilaments.

Two lines of evidence demonstrate that mitochondria accumulate in cytasters and move with them. First, egg loaded with mitotracker shows that ectoplasmic mitochondria form small moving clusters. Second, mitochondria loaded with a mitotracker colocalize with cytasters that have been labeled with fluorescent tubulin or actin.

The manner in which mitochondria and other organelles relate with the dynamic cytaster cytoskeleton is not yet understood and this is crucial to comprehend how they move together. The role of molecular motors and protein kinases in these processes is currently under investigation.

In this paper we show further evidence that the leech zygote is a highly compartmentalized cell that provides a detailed account of how different parts of the eukaryotic cell do their specific tasks in an integrated manner.

ACKNOWLEDGMENTS

We thank Víctor Guzmán, Rubén Peña, Víctor Monasterio, and José Arbildúa for technical assistance; Dr. John Nicholls for critical reading of the manuscript; and Dr. Duncan Stuart for important help in many phases of this work. This investigation was supported by Grant EDID 98-007, from the University of Chile, and Fondecyt 1991006.

REFERENCES

Abraham, V. C., Miller, A. L., Jaffe, L. F., and Fluck, R. A. (1993). Cytoplasmic microtubule arrays in *Oryzias latipes* (Medaka) eggs during ooplasmic segregation. *Biol. Bull.* **185,** 305–306.

Adams, A. E., and Pringle, J. R. (1984). Relationship of actin and tubulin distribution to bud growth in wild-type and morphogenetic-mutant *Saccharomyces cerevisiae. J. Cell Biol.* **98,** 934–945.

Astrow, S. H., Holton, B., and Weisblat, D. A. (1989). Teloplasm formation in a leech, *Helobdella triserialis,* is a microtubule-dependent process. *Dev. Biol.* **135,** 306–319.

Bassell, G. J., Powers, C. M., Taneja, K. L., and Singer, R. H. (1994a). Single mRNAs visualised by ultrastructural *in situ* hybridization are principally localized at actin filament intersections in fibroblasts. *J. Cell Biol.* **126,** 863–876.

Bassell, G. J., Singer, R. H., and Kosik, K. S. (1994b). Association of poly (A) mRNA with microtubules in cultured neurons. *Neuron* **12,** 571–582.

Bearer, E. L. (1992). Fluorescence microscopy of single actin filament labeled by conjugation to rhodamine. *Cell Dev. Biol.* **183,** 361–362.

Bearer, E. L., De Giorgis, J. A., Bodner, R. A., Kao, A. W., and Reese, T. S. (1993). Evidence for myosin motors on organelles in squid axoplasm. *Proc. Natl. Acad. Sci. USA* **90,** 11252–11256.

Boldogh, I., Vojtov, N., Karmon, S., and Pon, L. A. (1998). Interaction between mitochondria and the actin cytoskeleton in budding yeast requires two integral mitochondrial outer membrane proteins: Mmm1p and Mdm10p. *J. Cell Biol.* **141,** 1371–1381.

Bowerman, B. (1999). The maternal control of polarity and patterning during embryogenesis in the nematode *Caenorhabditis elegans. In* "Cell Lineage and Fate Determination" (S. A. Moody, Ed.), pp. 97–117. Academic Press, Canada.

Buendia, B., Antony, C., Verde, F., Bornens, M., and Karsenti, E. (1990). A centrosomal antigen localized on intermediate filaments and mitotic spindle pole. *J. Cell Sci.* **97,** 259–271.

Carminati, J. L., and Stearns, T. (1997). Microtubules orient the mitotic spindle in yeast through dynein-dependent interactions with the cell cortex. *J. Cell Biol.* **138,** 629–641.

Cottingham, F. R., and Hoyt, M. A. (1997). Mitotic spindle positioning in *Saccharomyces cerevisiae* is required for proper orientation of the mitotic spindle. *J. Cell Biol.* **127,** 129–138.

Davies, R. W., and Oosthuizen, J. H. (1993). A new species of duck leech from Northamerica formerly confused with *Theromyzon rude* (Rynchobdellida: Glossiphoniidae). *Can. J. Zool.* **71,** 770–775.

De Brabander, M., Geuens, G., Nuydens, R., Willebrords, R., and De Mey, J. (1981). Taxol induces the assembly of free microtubules in living cells and blocks the organizing capacity of the centrosome and kinetochores. *Proc. Natl. Acad. Sci. USA* **78,** 5608–5612.

Desai, A., Maddox, P. S., Mitchison, T. J., and Salmon, E. D. (1998). Anaphase A chromosome movement and poleward spindle microtubule flux occur at similar rates in *Xenopus* extract spindles. *J. Cell Biol.* **141,** 703–713.

Dirksen, E. R. (1961). The presence of centrioles in artificially activated sea urchin eggs. *J. Cell Biol.* **11,** 211–217.

Doyle, T., and Boekstein, D. (1996). Movement of yeast cortical actin cytoskeleton visualized *in vivo. Proc. Natl. Acad. Sci. USA* **93,** 3886–3891.

Fernández, J. (1980). Embryonic development of the glossiphoniid leech *Theromyzon rude:* Characterization of developmental stages. *Dev. Biol.* **76,** 245–262.

Fernández, J., and Stent, G. S. (1980). Embryonic development of the glossiphoniid leech *Theromyzon rude:* Structure and development of the germinal bands. *Dev. Biol.* **78,** 407–434.

Fernández, J., and Olea, N. (1982). Embryonic development of glossiphoniid leeches. *In* "Developmental Biology of Freshwater Invertebrates" (F. W. Harrison and R. R. Cowden, Eds.), pp. 317–361. A. R. Liss, New York.

Fernández, J., Téllez, V., and Olea, N. (1992). Hirudinea. *In* "Microscopic Anatomy of Invertebrates" (F. W. Harrison and S. L. Gardiner, Eds.), Vol. 7, pp. 323–394. Wiley–Liss, New York.

Fernández, J., Olea, N., and Téllez, V. (1994). Formation of the male pronucleus, organization of the first interphase monaster and establishment of the perinuclear plasm domain in the egg of the glossiphoniid leech *Theromyzon rude. Dev. Biol.* **164,** 111–122, doi:10.1006/dbio.1994.1184.

Fernández, J., and Olea, N. (1995). Formation of the female pronucleus and reorganization and disassembly of the first interphase cytoskeleton in the egg of the glossiphoniid leech *Theromyzon rude. Dev. Biol.* **171,** 541–553, doi:10.1006/dbio.1995.1303.

Fernández, J., Olea, N., Ubilla, A., and Cantillana, V. (1998a). Formation of polar cytoplasmic domains (teloplasms) in the leech egg is a three-step segregation process. *Int. J. Dev. Biol.* **42,** 149–162.

Fernández, J., Roegiers, F., Cantillana, V., and Sardet, C. (1998b). Formation and localization of cytoplasmic domains in leech and ascidian zygotes. *Int. J. Dev. Biol.* **42,** 1075–1084.

Gard, D. L., Hafezi, S., Zhang, T., and Doxsey, S. (1990). Centrosome duplication continues in cycloheximide-treated *Xenopus* blastulae in the absence of a detectable cell cycle. *J. Cell Biol.* **110,** 2033–2042.

Gard, D., Cha, B. J., and Schroeder, M. M. (1995). Confocal immunofluorescence microscopy of microtubules, microtubule-associated proteins, and microtubule-organizing centers during amphibian oogenesis and early development. *In* "Current Topics in Developmental Biology" (R. A. Pederson and G. P. Schatten, Eds.), Vol. 31, pp. 383–431. Academic Press, San Diego.

Glotzer, J. B., and Ephrussi, A. (1996). mRNA localization and the cytoskeleton. *In* "Seminars is Cell and Developmental Biology" (E. Karsenti, Ed.), Vol. 7, pp. 357–365, doi:10.1006/scdb.1996.0045. Academic Press, San Diego.

Grünert, S., and St. Johnston, D. (1996). RNA localization and the development of asymmetry during *Drosophila* oogenesis. *In* "Current Opinions Genetics and Development" (J. Kimble and J. Smith, Eds.), Vol. 6, pp. 395–402. Elsevier, London.

Hamill, D., Davis, J., Drawbridge, J., and Suprenant, K. A. (1994). Polyribosome targeting to microtubule preparation from sea urchin embryos. *J. Cell Biol.* **127,** 973–984.

Harris, P. J. (1981). Calcium regulation of cell cycle events. *In* "Mitosis/Cytokinesis" (A. M. Zimmerman and A. Forer, Eds), pp. 29–57. Academic Press, New York.

Harris, P. J., and Clason, E. L. (1992). Conditions for assembly of tubulin-based structures in unfertilized sea urchin eggs: Spirals, monasters and cytasters. *J. Cell Sci.* **102,** 557–567.

Hird, S. (1996). Cortical actin movement during the cell cycle of the *Caenorhabditis elegans* embryo. *J. Cell Sci.* **109,** 525–533.

Hyman, E., Drechsel, D., Kellogg, D., Salser, S., Sawin, K., Steffen, P., Wordeman, L., and Mitchison, T. (1991). Preparation of modified tubulins. *Methods Enzymol.* **196,** 478–485.

Inoué, S., and Salmon, E. D. (1995). Force generation by microtubule assembly/disassembly in mitosis and related movements. *Mol. Biol. Cell* **6,** 1619–1640.

Jeffery, W. R. (1995). Development and evolution of an egg cytoskeletal domain in ascidians. *In* "Current Topics in Developmental Biology" (R. A. Pederson and G. P. Schatten, Eds.), Vol. 31, pp. 243–276. Academic Press, New York.

Kallenbach, R. J. (1985). Ultrastructural analysis of the initiation and development of cytasters in sea urchin eggs. *J. Cell Sci.* **73,** 261–278.

Karsenti, E., Boleti, H., and Vernos, I. (1996). The role of microtubule dependent motors in centrosome movement and spindle pole organization during mitosis. *In* "Seminars in Cell and Developmental Biology" (E. Karsenti, Ed.), Vol. 7, pp. 367–378, doi:10.1006/scdb.1996.0046. Academic Press, San Diego.

Kemphues, K. J., and Strome, S. (1997). Fertilization and establishment of polarity in the embryo. *In* "*C. elegans* II," pp. 335–360. Cold Spring Harbor Laboratory Press, Plainview, NY.

Kilmartin, J. V., and Adams, A. E. M. (1984). Structural rearrangements of tubulin and actin during the cell cycle of the yeast *Saccharomyces. J. Cell Biol.* **98,** 922–933.

King, M. L. 1996. Molecular basis for cytoplasmic localization. *Dev. Genet.* **19,** 183–189.

Kube-Granderath, E., and Schliwa, M. (1997). Unusual distribution of γ-tubulin in the giant fresh water amoeba *Reticulomyxa filosa. Eur. J. Cell Biol.* **72,** 287–296.

Lechler, T., and Li, R. (1997). *In vitro* reconstitution of cortical actin assembly sites in budding yeast. *J. Cell Biol.* **138,** 95–103.

Li, R., Zeng, Y., and Drubin, D. (1995). Regulation of cortical actin cytoskeleton assembly during polarized cell growth in budding yeast. *J. Cell Biol.* **128,** 599–615.

Machesky, L. M. (1998). Cytokinesis: IQGAPs find a function. *In* "Current Biology" (P. Newmark, Ed.), Vol. 8, pp. R202–R205. Elsevier, London.

Mahajan-Miklos, S., and Cooley, L. (1994). Intercellular cytoplasm transport during *Drosophila* oogenesis. *Dev. Biol.* **165,** 336–351, doi:10.1006/dbio.1994.1257.

Maro, B., Howlett, S. K., and Webb, M. (1985). Non-spindle microtubule organizing centers in metaphase II-arrested mouse oocytes. *J. Cell Biol.* **101,** 1665–1672.

Mitchison, T. J., and Cramer, L. P. (1996). Actin-based cell motility and cell locomotion. *Cell* **84,** 371–379.

Monasterio, O., and Timasheff, S. N. (1987). Inhibition of tubulin self-assembly and tubulin-colchicine GTPase activity by guanosine 5′-(γ-fluorotriphosphate). *Biochemistry* **26,** 6091–6099.

Mulholland, J., Preuss, D., Moon, A., Wong, A., Drubin, D., and Botstein, D. (1994). Ultrastructure of the yeast cytoskeleton and its association with the plasma membrane. *J. Cell Biol.* **125,** 381–391.

Pardee, J. D., and Spudich, J. A. (1982). Purification of actin muscle. *Methods Enzymol.* **85,** 164–181.

Pereira, A., Dalby, B., Stewart, R. J., Doxsey, S. J., and Goldstein, L. S. B. (1997). Mitochondrial association of a plus end-directed microtubule motor expressed during mitosis in *Drosophila. J. Cell Biol.* **136,** 1081–1090.

Reverberi, G. (1971). Ascidian. *In* "Experimental Embryology of Marine and Freshwater Invertebrates" (G. Reverberi, Ed.), pp. 507–549. North Holland, Amsterdam/London.

Riparbelli, M. G., Stouthamer, R., Dallai, R., and Callaini, G. (1998). Microtubule organization during the early development of the parthenogenetic egg of the hymenopteran *Muscidifurax uniraptor. Dev. Biol.* **195,** 89–99, doi:10.1006/dbio.1997.8841.

Satoh, N. (1999). Cell fate determination in the ascidian embryo. *In* "Cell Lineage and Fate Determination" (S. A. Moody, Ed.), pp. 59–74. Academic Press, Canada.

Schatten, G., Simerly, C., and Schatten, H. (1985). Microtubule configuration during fertilization, mitosis and early development in the mouse. *Proc. Natl. Acad. Sci. USA* **82,** 4152–4156.

Schliwa, M. (1980). Structural organization of detergent-extracted cells. *In* "Proceedings of the 38th Meeting of Electron Microscopy Society of America" (G. W. Bailey, Ed.), pp. 814–817. Claitors, Baton Rouge, LA.

Schliwa, M., and van Blerkom, J. (1981). Structural interactions of cytoskeletal components. *J. Cell Biol.* **90,** 222–235.

Shimizu, T. (1982). Development of the freshwater oligochaete *Tubifex. In* "Developmental Biology of Freshwater Invertebrates" (F. W. Harrison and R. R. Cowden, Eds.), pp. 283–316. A. R. Liss, New York.

Shimizu, T. (1984). Dynamics of the actin microfilament system in the *Tubifex* egg during ooplasmic segregation. *Dev. Biol.* **106,** 414–426.

Shimizu, T. (1995). Role of the cytoskeleton in the generation of spatial patterns in *Tubifex* eggs. *In* "Current Topics in Developmental Biology" (D. G. Capco, Ed.), Vol. 31, pp. 197–235. Academic Press, Orlando.

Shimizu, T. (1997). Reorganization of the cortical cytoskeleton during maturation divisions in the *Tubifex* egg: Possible involvement of protein kinase C. *Dev. Biol.* **188,** 110–121, doi:10.1006/dbio.1997.8606.

St. Johnston, D., and Nüsslein-Volhard, C. (1992). The origin of pattern and polarity in the *Drosophila* embryo. *Cell* **68,** 201–219.

Svitnika, T. M., Verkhovsky, A. B., McQuade, K. M., and Borisy, G. G. (1997). Analysis of the actin-myosin II system in fish epidermal keratocytes: Mechanisms of cell body translocation. *J. Cell Biol.* **139,** 397–415.

Van Blerkom, J. (1991). Microtubule mediation of cytoplasmic and nuclear maturation during the early stages of resumed meiosis in cultured mouse oocytes. *Proc. Natl. Acad. Sci. USA* **88,** 5031–5035.

Waddle, J. A., Karpora, T. S., Waterston, R. H., and Cooper, J. A. (1996). Movement of cortical actin patches in yeast. *J. Cell Biol.* **132,** 861–870.

Waterman-Storer, C. M., and Salmon, E. D. (1997). Actomyosin-based retrograde flow of microtubules in the lamella of migrating epithelial cells influences microtubule dynamic instability and turnover and is associated with microtubule breakage and treadmilling. *J. Cell Biol.* **139,** 417–434.

Weisblat, D. A., Huang, F. Z., and Isaksen, D. E. (1999). Cell fate specification in glossiphoniid leech: Macromeres, micromeres and proteleoblasts. *In* "Cell Lineage and Fate Determination" (S. A. Moody, Ed.), pp. 185–205. Academic Press, Canada.

Weisenberg, R. C., Borisy, G. G., and Taylor, E. W. (1968). The colchicine-binding protein of mammalian brain and its relation to microtubules. *Biochemistry* **7,** 4466–4479.

Winter, D., Podtelejnikov, A. V., Mann, M., and Li, R. (1997). The protein complex containing actin-related proteins Arp2 and Arp 3 is required for the motility and integrity of yeast cortical actin patches. *In* "Current Biology"(P. Newmark, Ed.), Vol. 7, pp. 519–529. Elsevier, London.

Yeh, E. R., Skibbens, R. V., Cheng, J. W., Salmon, E. D., and Bloom, K. (1995). Spindle dynamics and cell cycle regulation of dynein in the budding yeast *Saccharomyces cerevisiae*. *J. Cell Biol.* **130,** 687–700.

Received for publication July 12, 2000
Revised September 7, 2000
Accepted September 7, 2000
Published online November 3, 2000